Margetts AR (ed.) (1977) *Hydro-acoustics in Fisheries Research*, A symposium held in Bergen, 19–22 June 1973, *Rapports et Proces-Verbaux des Reunions*, vol. 170. Copenhagen: International Council for the Exploration of the Sea.

Medwin H and Clay CS (1998) *Fundamentals of Acoustical Oceanography*. San Diego, CA: Academic Press.

Nakken O and Venema SC (eds) (1983) *Symposium on Fisheries Acoustics*, Selected papers of the ICES/FAO Symposium on Fisheries Acoustics, Bergen, Norway, 21–24 June 1982, FAO *Fisheries Report* no. 300. Rome: Food and Agriculture Organization of the United Nations.

Ona E (1990) Physiological factors causing natural variations in acoustic target strength of fish. *Journal of the Marine Biological Association of the United Kingdom*, 70: 107–127.

Physics of Sound in the Sea (1969) Reprint of the 1946 edition. Washington, DC: Department of the Navy.

Progress in Fisheries Acoustics (1989) *Proceedings of the Institute of Acoustics*, vol. 11, no. 3. St. Albans: Institute of Acoustics.

Simmonds EJ and MacLennan DN (eds) (1996) *Fisheries and Plankton Acoustics*, Proceedings of an ICES international symposium held in Aberdeen, Scotland, 12–16 June 1995. *ICES Journal of Marine Science*, vol. 53, no. 2. London: Academic Press.

Urick RJ (1983) *Principles of Underwater Sound*, 3rd edn. New York: McGraw-Hill.

ACOUSTICS, ARCTIC

P. N. Mikhalevsky, Science Applications International Corporation, McLean, VA, USA

doi:10.1006/rwos.2001.0314

Introduction

The Arctic Ocean is an isolated mediterranean basin with only limited communication with the world's oceans, principally the Atlantic Ocean via the Fram Strait and the Barents Sea, and the Pacific Ocean via the Bering Strait. The ubiquitous feature of the Arctic Ocean is the sea ice that covers the entire Arctic basin during the winter months and only retreats off the shallow water shelf areas in the summer months, creating a permanent cap over most of the central Arctic basin (**Figure 1**) (*see* **Sea Ice: Overview**). The presence of the year-round sea ice cover determines the unique character of acoustic propagation and ambient noise in the Arctic Ocean. The sea ice insulates the Arctic Ocean from solar heating in the summer months, creating a year-round upward refracting sound speed profile with the sound speed minimum at the water–ice interface (*see* **Acoustics, Deep Ocean**). Sound, therefore, is refracted upward and is continuously reflected from the ice as it propagates, causing attenuation by scattering, mode conversion, and absorption that increases rapidly with frequency. The lack of solar forcing and the Arctic Ocean's restricted communication with the other oceans of the world creates a very stable acoustic channel with significantly reduced fluctuations of acoustic signals in comparison with the temperate oceans. In contrast to the central basin, acoustic propagation on the Arctic shelves and in the marginal ice zones (MIZs, those areas between the average ice minimum and maximum) (**Figure 1**), is quite complex and variable owing to the seasonal retreat of the sea ice, river run-off, and bottom interaction (*see* **Acoustics, Shallow Water; Acoustics in Marine Sediments**).

Over the last half-century Arctic acoustics research and development has largely supported submarine operations. The importance of the Northern Sea Route to the Soviet Union, and the prospect of Soviet nuclear ballistic missile submarines exploiting the unique Arctic acoustic environment to remain undetected provided the need for this research. Since the end of the Cold War and the beginning of concern about 'global warming' there has been a new focus for Arctic acoustics on acoustic thermometry and acoustic remote sensing (*see* **Tomography**). The Arctic Ocean is the world's 'air-conditioner', maintaining the surface heat balance, and it provides fresh water to the world's oceans, principally in the form of sea ice discharged from the Fram Strait. The latter regulates convective overturning in the Greenland and Norwegian Seas that in turn drives the global thermohaline circulation with significant impact on climate. Monitoring changes in the temperature and stratification of the Arctic Ocean and sea ice thickness using acoustics is an important capability that will improve our understanding of the Arctic Ocean and its role in global climate change.

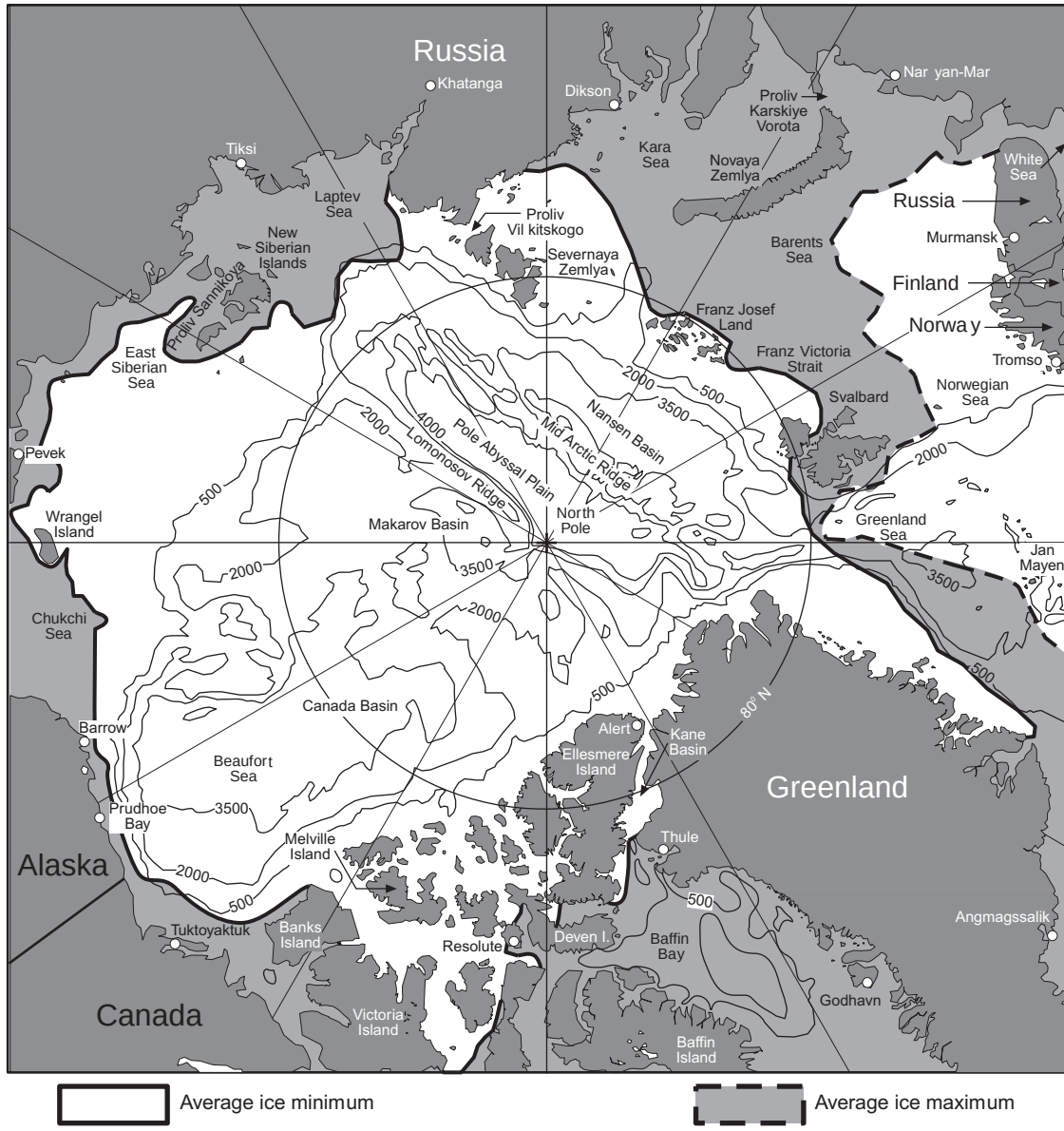

Figure 1 Map of the Arctic Ocean showing the average minimum and maximum sea ice extent, as well as the major bathymetric features, and other significant geographic locations.

History

The first large program dedicated to acoustics research in the Arctic Ocean was undertaken by the US Navy Underwater Sound Laboratory, as it was then known, in 1958 in connection with the International Geophysical Year. Also in that year the US nuclear submarine *Nautilus* (SSN 571) made its historic voyage to the North Pole, marking the beginning of regular submarine operations in the Arctic Ocean. From 1958 to 1975 the USA conducted much of its acoustics research from manned ice islands (thick tabular sections of land-fast ice that occasionally break away from the Ellesmere ice shelf) that remained within the polar pack ice (see Cryosphere: Sea Ice). The most famous of these was Fletcher's Ice Island, also known as T3, which was discovered in June 1950. T3, originally 14.5 km long, 6.4 km wide and 52 m thick, provided an ideal platform for Arctic research including acoustics. The first experiments in 1958 were aimed at investigating the feasibility of using the RAFOS (Ranging and Fixing of Sound) for submarine navigation in Arctic waters. Explosive signals were deployed from T3 and other ice stations while the *USS Skate* (SSN 578) attempted to receive the signals for acoustic

crossfixing. While RAFOS was never operationally deployed, a significant amount was learned about the upward refracting sound speed profile, propagation, and resulting scattering losses, as well as ambient noise and reverberation.

The Soviet Union operated at least two manned year-round ice stations in the Arctic continuously from 1937 through 1992. In 1971 they began POLEX (Polar Experiment), which was an intense set of oceanographic, ice, and atmospheric measurements over the entire Arctic Ocean basin that continued for a decade. From 1971 through 1994 the US Office of Naval Research sponsored or co-sponsored many international acoustic-related research science programs based from seasonal ice camps in the Arctic, staged out of facilities in Alaska, Canada, Greenland, and Svalbard. These included the Arctic Ice Dynamics Experiments (AIDJEX), 1971–76; the FRAM and MIZEX series in the central Arctic basin and marginal ice zones respectively, 1979–87; the Coordinated East Arctic Experiment (CEAREX), 1988–89; the Sea Ice Mechanics Initiative (SIMI), 1993–94; and the Transarctic Acoustic Propagation Experiment (TAP) in 1994. These programs quantified sea ice properties and ice scattering processes, bottom and surface reverberation, Arctic plate tectonics with seismic reflection and refraction, identified the mechanisms of ice generated ambient noise, discovered the exceptional phase stability of low frequency propagation ($\sim$20–30 Hz), and demonstrated the feasibility of basin scale acoustic thermometry in the Arctic Ocean.

The US, UK, and Soviet Union (now Russia) have operated submarines in the Arctic Ocean and conducted a significant amount of acoustics research. In particular, the US Navy's Submarine Ice Exercises (SUBICEXs) were conducted over almost three decades by the Arctic Submarine Laboratory (ASL) under the leadership of Dr Waldo Lyon, often in conjunction with seasonal ice camps. Dr Lyon was one of the first to investigate propagation in polar stratified waters, beginning shortly after the end of World War II, working with Canadian researchers. From the Naval Electronics Laboratory (NEL) in San Diego, Dr Lyon led the development of upward-looking ice profiling sonar, and the forward-looking ice avoidance sonar, that proved critical for safe under-ice submarine operations. SUBICEXs were designed to test all aspects of submarine operations including surfacing through ice, and weapons effectiveness (see *Under Ice* in Further Reading). In 1993 the US Navy supported a dedicated 60 day science cruise in the Arctic with the *USS Pargo* (SSN 650). This started the Submarine Science Ice Expeditions (SCICEX) that were conducted each year from 1995 to 1999. These multidisciplinary cruises have confirmed the large changes in the Arctic Ocean thermohaline structure, including the warming of the Arctic Intermediate Water (AIW, see below) that was measured acoustically during the TAP experiment in 1994. Other data and modeling have shown strong evidence of decadal Arctic oscillations, but longer observational time series are needed (*see* **North Atlantic Oscillation (NAO)**). A trans-basin acoustic section was started in October 1998 from a source located in the Franz Victoria Strait to a receiving array in the Lincoln Sea. This 3-year US/Russian collaborative effort is expected to be followed by more permanent long-term monitoring of the Arctic Ocean using acoustics.

Arctic Ocean Sound Speed Structure

The structure of the typical sound speed profile in the Arctic consists of components that correspond closely to the primary stratified water masses of the Arctic Ocean (**Figure 2**) (*see* **Arctic Basin Circulation. Water Types and Water Masses**). The uppermost layer is Polar Water (PW) defined by temperatures $< 0^{\circ}$C and salinities < 34.5 ppt and extends from the surface to depths of 100–200 m. There is often a mixed layer of Polar Water 30–60 m thick just below the ice with a nearly constant temperature near the freezing point and nearly constant salinity at around 33.6 ppt (*see* **Arctic Basin Circulation**). Below the mixed layer the temperature and salinity increase uniformly, attaining 0°C and 34.5 ppt respectively, at the base of the Polar Water layer. Arctic Intermediate Water (AIW) – also known as the Atlantic Layer reflecting its origin (and sometimes referred to as Atlantic Intermediate Water) – is defined by temperatures $> 0^{\circ}$C and salinities > 34.5 ppt and extends from the base of the Polar Water to a depth of 1000 m. Temperature increases with depth through the AIW layer to a maximum at approximately 200–500 m depth and then decreases with depth to 0°C at about 1000 m. AIW enters the Arctic Ocean via the West Spitzbergen Current from the Fram Strait and via the Barents Sea east of Franz Josef Land (see Ocean Currents: Arctic Basin Circulation). The shallower depths (200 m) of the temperature maximum of the AIW occur in the eastern Arctic and approaches 2°C. This temperature maximum deepens to 500 m the western Arctic in the Canada Basin and is approximately 0.4°C. Salinity increases with depth in the AIW layer from 34.5 ppt to 34.9 ppt at about the same depth of the temperature maximum and remains constant at 34.9 ppt below this depth. Deep

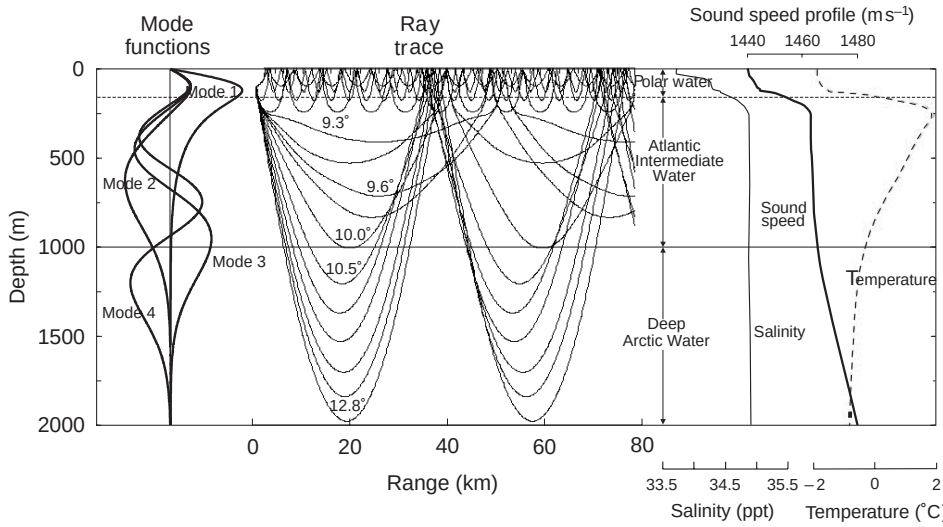

Figure 2 The Arctic sound speed profile shown on the right was computed from the measured temperature and salinity, also shown, from an ice camp in the eastern Arctic Ocean in April 1994. A ray trace for this sound speed profile is plotted for a source at a depth of 100 m. The mode shapes computed at 20 Hz using this profile are shown on the left. The major Arctic water masses (see text) are indicated.

Arctic Water (DW) is a relatively homogeneous water mass from a depth of 1000 m to the bottom, with temperatures $< 0°C$ and a nearly constant salinity of 34.9 ppt.

The resulting sound speed profile (**Figure 2**) for these typical deep Arctic basin conditions has a minimum at the ice–water interface of 1435–1440 m s^{-1} and increases with depth to the bottom. In the near-surface mixed layer of the PW the sound speed gradient is $+0.016\,s^{-1}$, due entirely to the increase of pressure with depth, as temperature and salinity are constant. Below the mixed layer the sound speed increases rapidly with the increasing temperature and salinity (temperature having the far dominant effect) to the depth of the maximum temperature in the AIW layer with gradients of $+0.1\,s^{-1}$ or more, reaching a sound speed between 1455 and 1465 m s^{-1}. Below the depth of the AIW temperature maximum the sound speed continues to increase, but with reduced gradients of $+0.01\,s^{-1}$ or less as the temperature decreases, but the pressure increases and the salinity is constant. Below 1000 m in the DW both temperature and salinity are nearly constant and the sound speed continues to increase with the $+0.016\,s^{-1}$ gradient to the bottom associated with the increasing pressure.

In general the Arctic or polar profile can be characterized (and is often approximated) roughly as a bilinear upward refracting profile with the large positive gradient at the near surface creating a strong near-surface duct and a smaller positive gradient below this 'knee' to the bottom. This structure is important to understanding the resulting propagation effects described below. There are both regional and temporal variations of this typical sound speed structure associated with the corresponding variations in the water masses described above. The strong positive gradient associated with the upper AIW layer weakens as the 'knee' in the sound speed profile (**Figure 2**) deepens from 200 m to about 500 m as one moves from the eastern Arctic Ocean near Svalbard (where the profile in **Figure 2** was measured) into the western Arctic Ocean and the Beaufort and Chukchi Seas. In the Beaufort and north Chukchi Seas the influx of warmer Bering Sea water can create a sound speed maximum just below the mixed layer of the PW at depths between 50 and 80 m, creating a double duct. Because of the year-round ice cover, seasonal, interannual, and recently identified decadal time scales dominate the temporal variations of the sound speed profile. The seasonal and interannual variability is confined almost entirely to the PW layer. The decadal variability is seen in the PW and AIW layers. Mesoscale and internal wave dynamics are approximately one order of magnitude less energetic in the Arctic Ocean than in the temperate seas and so have a small influence on the sound speed profile and this results in the exceptional signal stability at low frequencies (discussed below).

Propagation

Acoustic propagation in the Arctic is dominated by the repeated reflection of the sound from the sea ice as illustrated in **Figure 2**. The ray trace shown was

Figure 3 A photograph of the pack ice in the central Arctic Ocean taken at the FRAM II Ice Camp in May 1980. A weathered pressure ridge is shown on the left bounding a relatively flat multi-year ice floe on the right that is typical of the central arctic. The blocks of ice in the foreground are 3–4 m high. (Photo by P. Mikhalevsky.).

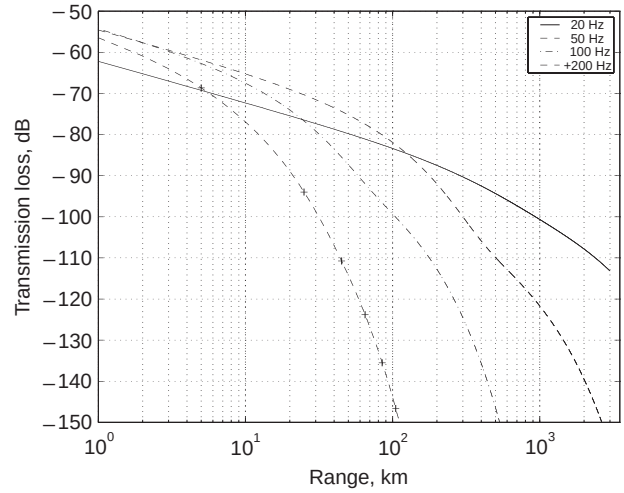

Figure 4 The transmission loss plotted as a function of range for 20, 50, 100, and 200 Hz. The source and receiver were located at 60 m depth. The ice was modeled as a rough elastic plate including statistical parameters for the upper and lower side of the ice representative of the ice floe and ridge structure typical of the central Arctic.

computed using the sound speed profile of **Figure 2**. The morphology of sea ice is quite complicated in general (*see* **Sea Ice: Overview**). **Figure 3** is a photograph taken in the pack ice at an ice camp in the eastern Arctic. It shows a typical pressure ridge on the left that forms between two ice floes when winds and currents compress the pack. Pressure ridges can extend as much as several tens of meters below the ice, and consist of unconsolidated blocks in newly formed ridges as well as refrozen consolidated structures in older ridges. In general the sea ice in the Arctic consists of relatively smooth floes (the right part of **Figure 3**) laced with pressure ridges and/or open leads as the pack works between convergent and divergent conditions. Average ice roughness and thickness measurements derived from upward-looking submarine sonars have historically (1958–76) been in the range of 1–5 m rms and 2–4 m respectively[1]. Recent analysis of SCICEX data (1993–97), however, has shown that since the late 1970s the ice has thinned by as much as 40%[2], which would also imply a reduction in ice roughness as well. The thicker ice and correspondingly greater roughness is typically found in the eastern Arctic and just north of the eastern Canadian Archipelago and Greenland, where the transpolar drift pushes the ice.

The acoustic energy is reflected and scattered from the rough ice and converted to both shear waves and compressional waves within the ice, resulting in significant frequency-dependent attenuation loss. Because of this, trans-basin propagation in the Arctic is limited to frequencies typically below 30 Hz or wavelengths exceeding about 50 m. **Figure 4** shows the propagation loss plotted as a function of range for several frequencies. The curves in **Figure 4** were generated using a model that includes a rough elastic plate representing the ice cover, with a two scale roughness spectrum that models pressure ridges and the smoother intervening floes[3]. The model includes the statistics for both the underside and surface of the ice since at lower frequencies as the wavelength becomes much greater than the ice thickness the reflection occurs at the ice–air interface. Submarine ice draft statistics from the eastern Arctic over the Nansen Basin (**Figure 1**) were used for **Figure 4**. As **Figure 4** shows the Arctic acoustic waveguide is a low pass filter. So much so in fact that in comparison with propagation in the temperate oceans which scatter from surface waves that have a similar roughness spectrum, at a given range, equivalent propagation loss in the Arctic requires transmitting at a frequency as much a factor of ten less.

On the left side of **Figure 2** the acoustic mode shapes for modes 1–4 at 20 Hz are plotted for the

[1] LeSchack LA (1980) *Arctic Ocean Sea-ice Statistics Derived from Upward-Looking Sonar Data Recorded during Five Nuclear Submarine Cruises*. Technical Report to ONR under Contract N00014-76-C-0757/NR 307-374. Maryland, LeSchack Associates, Ltd.

[2] Rothrock DA, Yu Y and Maykut GA (1999) Thinning of the arctic sea-ice cover. *Geophysical Research Letters* 26(23): 3469–3472.

[3] Kudryashov VM (1996) Calculation of the acoustic field in an arctic waveguide. *Physical Acoustics*. 42: 386–389.

profile shown. The acoustic modes can be thought of as the interference pattern of upward and downward going acoustic rays (**Figure 2**) whose turning depths (the depth where the rays are horizontal) correspond with the depth of the deepest peak of the mode amplitude (*see* **Acoustics, Deep Ocean**). At 20 Hz, mode 1 consists of those paths that are trapped in the strong near-surface duct created by the thermocline in the transition from the PW to AIW. The higher modes correspond to rays with greater launch angles that turn at successively deeper depths in the Arctic Ocean. Rough surface scattering theory tells us that the loss per bounce or reflection increases with grazing angle and frequency (i.e., the steeper rays, or higher modes have greater loss per bounce). However, even though the lower modes (lower grazing angles) have lower per bounce loss, those that are trapped in the upper duct experience many more interactions with the ice, as clearly seen in **Figure 2**, and consequently their net loss per kilometer is higher. At shorter ranges for a source and receiver in the upper duct (**Figure 4**) the propagation is dominated by the lower modes (or equivalently the lower grazing angle rays that are trapped), but these get stripped away as the range increases and at longer ranges ($>$100–200 km) the higher modes (or equivalently the higher grazing angle rays that are not trapped) dominate. Because the source and receiver are shallow (at 60 m depth) for the model run in **Figure 4**, there is a less efficient excitation of mode 1 at 20 Hz (i.e., destructive interference with the surface reflected energy) than at the higher frequencies. Thus less of the energy is trapped in the near-surface duct. This results in lower energy being received on the shallow receiver at closer ranges and hence the higher initial propagation loss at 20 Hz. As the frequency increases the mode shapes tend to compress toward the surface (because the wavelength is getting smaller). For a shallow source more of the energy is trapped in this upper duct at higher frequencies (see discussion of frequency dispersion and **Figure 6** below). Given the higher per bounce losses at the higher frequencies, and the greater number of bounces experienced by these trapped modes, it can be seen why attenuation in the Arctic increases rapidly with frequency. For deeper sources the near-surface duct is not as important and higher grazing angle (higher mode) propagation and loss are dominant at all ranges; however, the higher loss per bounce at higher frequencies still results in more rapid attenuation as the frequency increases.

There is a significant body of research on the scattering and reverberation of acoustic energy from the sea ice. The earliest models relied on rough free surface scattering theory with empirical fits to important parameters such as rms ice roughness and average ridge spacing. The free surface scattering models that included ridge-like morphology performed reasonably well at frequencies from 250 Hz to 2000 Hz. At lower frequencies they tended to underpredict the loss. When elastic coupling and scattering into the ice (particularly conversion to shear waves and the attenuation in the ice) are included, better agreement at the low frequencies has been achieved. In particular the ice keels and their spacing are important in the conversion of acoustic compressional waves into flexural modes in the ice. Le Page and Schmidt (*see* Further Reading) have shown that the intensity of acoustic scattering into the flexural modes of a rough ice plate strongly depends on the width of the roughness spatial spectra. In order to achieve consistent agreement with data the propagation loss models have become more complex, demanding additional input data, particularly about the structure of the sea ice and its constitutive properties.

Bottom interaction must also be included, for those paths which cross major features like the Lomonosov Ridge, and propagation on the arctic shelves (**Figure 1**). The Lomonosov Ridge can rise to 1500 m below the surface. **Figure 2** shows that modes 5 and higher (rays >11–12°) will start to interact with this feature and will begin to get stripped away for long-range propagation. As the frequency decreases below 20 Hz the modes tend to expand away from the surface and finally all modes will begin to interact with the bottom except in the very deepest parts of the Arctic basin. This leads to a lower frequency bound at 5–10 Hz for efficient long-range propagation. However, for high source levels at these frequencies there is significant backscatter reverberation from these bathymetric features that can be detected and mapped. Excellent correlation with known Arctic bathymetry as well as the discovery of uncharted features at basin scale ranges (1000 km) has been achieved using large explosive sources deployed from the ice. Over the shelves the shallow water propagation dictates bottom and surface/ice interaction at all frequencies; however, there are optimal propagation frequencies similar to deep water that depend upon the depth and boundary properties.

The stable upward refracting Arctic sound speed profile causes a very predictable modal and frequency dispersion. As can be seen in **Figure 2**, successively higher modes are propagating at higher sound speeds corresponding to higher group velocities. As a consequence at a given range, mode 1 arrives last, preceded in order by modes 2, 3, 4,

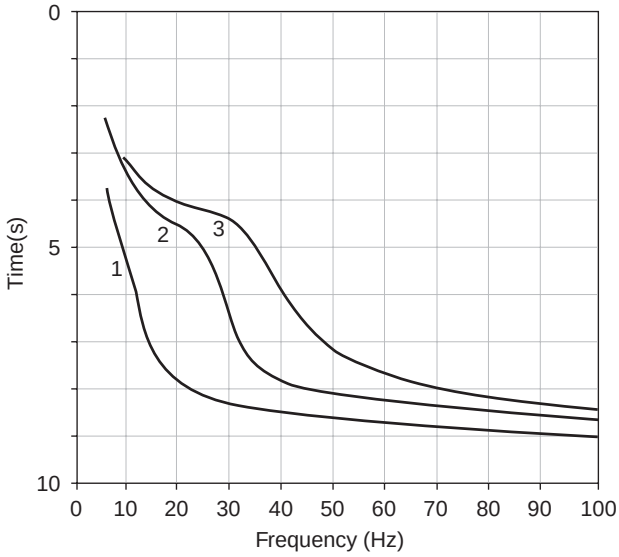

Figure 5 The arrival time of a broadband acoustic pulse plotted as a function of frequency showing the modal dispersion with mode 1 arriving last, preceded by modes 2 and 3 respectively. The absolute travel time can be obtained by adding 396.5 s to the time shown on the vertical axis. This modeled result agreed very closely with the received data. (Adapted with permission from DiNapoli *et al.,* 1978, in Von Winkle, 1984.)

etc. This can be observed by transmitting a wideband waveform such as an impulsive or explosive source and plotting the signal intensity as a function of frequency and time. **Figure 5** shows the arrival time from the computed group velocities of modes 1–3 for an explosive shot at a range of approximately 580 km in the Beaufort Sea. Although not plotted, this calculation agreed very closely with the measured data. Note also from **Figure 5** that as the frequency increases (as described above), the modes compress towards the surface and first mode 1, then mode 2 and finally mode 3 become trapped in the slower near-surface duct, as evidenced by the longer travel times. This modal dispersion and arrival pattern is a classic Arctic acoustic result. The data upon which **Figure 5** is based were taken in 1962; 32 years later in 1994 the TAP experiment measured the same arrival pattern, attesting to the very long-term stable water mass structure in the Arctic Ocean. Observations of the changes in the arrival times of these modes are directly related to the temperature changes of these water masses (since sound speed increases approximately 5 m/s per 1°C). In particular, at 20 Hz mode 2 is most sensitive to temperature changes in the AIW, as can be seen from **Figure 2**. A decrease in the travel time of mode 2 by 2 s was the indicator of the warming in the AIW observed in the 1994 TAP experiment (*see* **North Atlantic Oscillation (NAO)**).

In addition to the long-term stability of the Arctic sound speed profile, the short-term stability results in exceptional amplitude (~ 1 dB rms) and phase stability (~ 0.01 cycles rms) of acoustic signals at low frequencies even over ranges approaching 3000 km for up to 1 h (the longest continuous observations made to date). This applies to essentially fixed terminals. This was first observed in 1980 at 15–30 Hz and 300 km and then again in 1994 and 1999 at 20 Hz and 2700 km. This implies that coherent integration of up to 1 h with optimal gain is achievable (and has been demonstrated).

At very high frequencies (more than tens of kHz) reflection occurs at the ice–water interface. Attenuation is rapid, due not only to the severe scattering from the ice, but to volumetric absorption as well. These frequencies are used for short-range applications including the upward-looking ice profiling sonar, forward-looking ice avoidance sonar, and downward-looking depth sounders and bottom-mapping sonar. Torpedoes also operate at these frequencies and ice capture can be a problem, but Doppler processing can distinguish moving targets from the stationary ice (*see* **Sonar Systems**).

Ambient Noise

The ambient noise in the Arctic is highly variable, exhibiting some of the quietest as well as the noisiest ocean noise conditions of all the world's oceans. A composite of various measurements of Arctic ambient noise is shown in **Figure 6**. In **Figure 6**, Knudsen Sea State Zero refers to the ambient noise level in the temperate oceans at sea state zero (the quietest conditions) for comparison (*see* **Acoustic Noise**). Ice-generated ambient noise is the dominant mechanism contributing to the general character of ambient noise in the Arctic Ocean from a few tenths of Hz up to 10 000 Hz. Episodic noise is also present in the form of seismic events, such as earthquakes along the Mid Arctic Ridge (**Figure 1**), biologics (mostly marine mammals in the marginal ice zones), and man-made noise from ice breakers, and seismic exploration.

Ice noise is generated when the sea ice deforms, fractures, and breaks in response to environmental forcing such as wind, current, thermal, and internal and surface wave-induced stresses. In general, during stable or warming temperature conditions with low winds the quietest conditions obtain, particularly under shore-fast ice. During periods of rapid cooling ice-fracturing events resulting from thermal-induced tensile stresses can lead to higher noise levels. Higher noise levels also occur in the pack ice when the ice is in motion due to nonthermal forcing

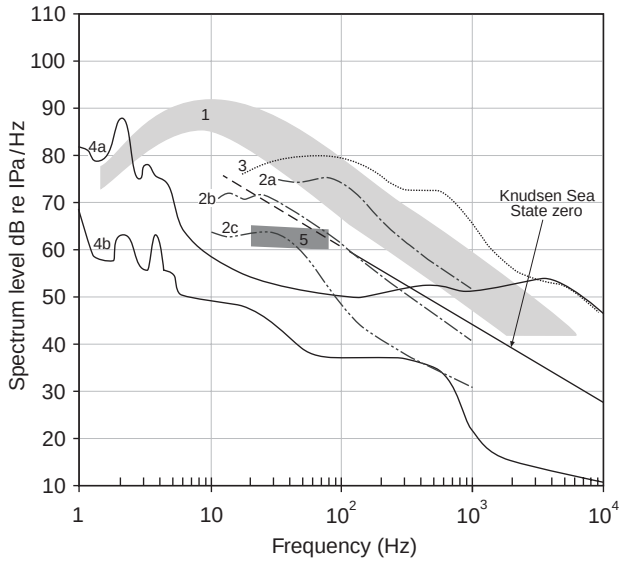

Figure 6 A composite of various measurements of Arctic ambient noise. (1) Central Arctic pack ice Nansen Basin, first- and multi-year floes, 2–3 m thick, with ridging, April 1982. (Reproduced with permission from Dyer, 1984.) (2) Beaufort Sea, summer and fall conditions: (a) highest levels observed, (b) typical cold weather situation following rapid temperature drop and thermal-induced cracking, (c) quietest conditions during warmer stable temperature periods with low winds September–October, 1961 and May–September 1962. (Reproduced with permission from DiNapoli *et al.*, 1978, in Von Winkle, 1984.) (3) Shore-fast ice in the Canadian Archipelago, winter conditions, thermal cracking, February 1963. (Reproduced with permission from Milne AR and Ganton JH (1964) Ambient noise under Arctic-Sea ice. *Journal of the Acoustic Society of America* 36(5): 855–863.) (4) Shore-fast ice in the Canadian Archipelago, spring conditions: (a) noisiest conditions observed during diurnal cooling, (b) quietest conditions observed during diurnal warming, April 1961 (Milne and Ganton 1964). (5) Chukchi Sea, spring conditions, cold stable temperatures, low winds, April 1999 (Mikhalevsky, APLIS Ice Camp).

such as high winds causing bumping, grinding and rubbing of the ice flows. In the marginal ice zone where the ice concentrations are typically less than in the central Arctic pack, ice concentration and surface gravity wave-induced flexural floe failure are the primary correlates with the ambient noise. The actual noise-generating mechanics are complicated but fall into at least two general categories. In the low frequency range (5–100 Hz) the important noise-generating mechanism is the unloading motion of the ice immediately following breaking. This has been shown to have a dipole radiation characteristic. The breaking process itself is important at intermediate frequencies (100–2000 Hz) and has an octopole radiation characteristic likely resulting from a slip–dislocation process.

Noise from earthquakes and other seismic events occur with some regularity within the Arctic Ocean, concentrated along the Mid Arctic Ridge (**Figure 1**). These events have been recorded on acoustic arrays suspended from the ice within approximately 300 km of the Mid Arctic Ridge. The received frequencies are typically 20 Hz and below. Earthborne acoustic pressure and shear waves emanate from the source and couple through the ocean floor above the epicenter to compressional waterborne waves that propagate vertically and are reflected from the ice canopy into the Arctic sound channel. Most of the energy from these events arrives via this path, but there are weaker precursors associated with crustal propagating compressional and shear waves that couple to the water directly below the receive array. These arrivals are easily identified by their vertical arrival angle at the array as well as their arrival time (*see* **Seismic Structure**).

Biological noise in the Arctic is concentrated in the marginal ice zones and near the edge of the pack ice. The bowhead is the most numerous of the baleen whales in Arctic waters, migrating along the coast of Alaska in the Chukchi and Beaufort Seas in the spring and then exiting the Arctic waters in the fall. They can vocalize from 25 to 3500 Hz, but their dominant frequencies are between 100 and 400 Hz. Of the toothed whales the beluga and narwhal are the most common, with calls ranging from a few hundred Hz to as high as 20 kHz. Many species of pinnipeds, including hair seals such as the bearded, hooded, harp, ringed, and ribbon seal, and the walrus frequent the marginal ice zones. As a group their calls typically range from a few hundred Hz to 10 kHz (see Marine Mammals).

Unlike the temperate oceans where shipping typically dominates the ambient noise spectrum, man-made noise in the Arctic is a small contributor except for specific events that are isolated in time and space. Such events include icebreakers, seismic exploration, and some military and experimental activities. Icebreaker noise peaks in the 50–100 Hz range, but with broadband contributions up to 1000 Hz. Seismic exploration occurs during the summer and fall seasons when the ice extent is minimum (**Figure 1**), allowing easier access to the shelves. Most of the activity has been confined to the Beaufort Sea off the North Slope of Alaska near Prudhoe Bay.

Conclusions

The presence of the year-round ice cap creates the upward refracting sound speed profile in the Arctic Ocean with the sound speed minimum at the ice–water interface. Reflection, scattering, mode conversion, and absorption by the rough elastic sea

ice cover causes high attenuation as frequency increases, limiting long-range propagation to very low frequencies. Bathymetric effects are important near the major ocean ridges, basin margins, and on the shelf areas where significant mode coupling can occur. The Arctic sound channel is very stable and predictable in the central Arctic basins and there is a close correspondence of propagating acoustic modes with the major water masses of the Arctic Ocean, especially the important AIW. This latter fact makes the use of acoustic thermometry for monitoring long-term Arctic Ocean temperature change particularly suitable. Ongoing research is exploring ways to relate changes in acoustic travel time and intensity to monitor other important variables in the Arctic Ocean including changes in the PW, DW, and the halocline, and average sea-ice thickness and roughness. The latter measurements, when combined with sea ice extent from satellite remote sensing, could provide an estimate of sea ice mass in the Arctic (*see* **Satellite Passive Microwave Measurements of Sea Ice**).

The role of the Arctic Ocean in shaping and responding to global climate change is only beginning to be explored. Cost-effective, long-term, year-round synoptic observations in the Arctic Ocean require new measurement strategies. The year-round ice cover in the Arctic prevents the use of satellites for direct ocean observations common in the ice-free oceans. Shore-cabled mooring-based observations using advanced biogeochemical sensors and acoustic sources and hydrophone arrays, as well as instrumented autonomous underwater vehicles (AUVs) and under-ice drifters, represent new approaches for observing the Arctic Ocean (*see* **Autonomous Underwater Vehicles (AUVs)**). Interestingly the RAFOS concept (using nonexplosive sources) is being evaluated anew as a way to track AUVs and drifters in the Arctic as well as for acoustic communication of data. It is clear that Arctic acoustics will have as large a role to play in this important new endeavor in the future, as it has had in the submarine and military operations of the past.

See also

Acoustics, Arctic. Acoustics in Marine Sediments. Acoustic Noise. Acoustics, Shallow Water. Arctic Basin Circulation. Autonomous Underwater Vehicles (AUVs). Bioacoustics. Ice–Ocean Interaction. Nepheloid Layers. North Atlantic Oscillation (NAO). Satellite Passive Microwave Measurements of Sea Ice. Sea Ice: Overview; Variations in Extent and Thickness. Seals. Seismic Structure. Thermohaline Circulation. Tomography. Under-ice Boundary Layer. Water Types and Water Masses.

Further Reading

Dyer I (1984) Song of sea ice and other Arctic Ocean melodies. In: Dyer I and Chryssostomidis C (eds) *Arctic Technology and Policy*, 11–37. Washington, DC: Hemisphere Publishing.

Dyer I (1993) Source mechanisms of Arctic Ocean ambient noise. In: Kerman BR (ed.), *Natural Physical Sources of Underwater Sound*, 537–551. Netherlands: Kluwer Academic.

Leary WM (1999) *Under Ice*. College Station: Texas A&M University Press.

LePage K and Schmidt H (1994) Modeling of low-frequency transmission loss in the central Arctic. *Journal of the Acoustic Society of America* 96(3): 1783–1795.

Mikhalevsky PN, Gavrilov AN and Baggeroer AB (1999) The transarctic acoustic propagation experiment and climate monitoring in the Arctic. *IEEE Journal of Oceanic Engineering* 24(2): 183–201.

Newton JL (1989) Sound speed structure of the Arctic Ocean including some effects on acoustic propagation. *US Navy Journal of Underwater Acoustics* 39(4): 363–384.

Richardson WJ, Greene CR Jr, Malme CI and Thomson DH (1995) *Marine Mammals and Noise*. San Diego: Academic Press.

Urick RJ (1975) *Principles of Underwater Sound*. New York: McGraw-Hill.

Von Winkle WA (ed.) (1984) *Naval Underwater Systems Center (NUSC) Scientific and Engineering Studies: Underwater Acoustics in the Arctic*. New London: Naval Underwater Systems Center Publisher.

ACOUSTICS, DEEP OCEAN

W. A. Kuperman, Scripps Institution of Oceanography, University of California, San Diego, CA, USA

doi:10.1006/rwos.2001.0312

Introduction

The acoustic properties of the ocean, such as the paths along which sound from a localized source will travel, are mainly dependent on its sound speed structure. The sound speed structure is dependent